Structure of NaI ion pairs in water clusters

ARTICLE *in* CHEMICAL PHYSICS · AUGUST 2000

Impact Factor: 1.65 · DOI: 10.1016/S0301-0104(00)00106-3

3 AUTHORS, INCLUDING:

Branka M. Ladanyi
Colorado State University
152 PUBLICATIONS **5,145** CITATIONS
SEE PROFILE

James Hynes
University of Colorado Boulder
304 PUBLICATIONS **17,462** CITATIONS
SEE PROFILE

ELSEVIER

Chemical Physics 258 (2000) 201–224

Chemical Physics

www.elsevier.nl/locate/chemphys

Structure of NaI ion pairs in water clusters

Gilles H. Peslherbe [a], Branka M. Ladanyi [b,*], James T. Hynes [c,d]

[a] *Department of Chemistry and Biochemistry, Concordia University, Montréal, Qué., Canada H3G 1M8*
[b] *Department of Chemistry, Colorado State University, Fort Collins, CO 80523, USA*
[c] *Department of Chemistry and Biochemistry, University of Colorado, Boulder, CO 80309-0215, USA*
[d] *Département de Chimie, CNRS UMR 8640, École Normale Supérieure, 24, rue Lhomond, 75213 Paris, France*

Received 18 January 2000

Abstract

The structural properties of the thermodynamically stable NaI salt ion pairs in water clusters have been investigated by means of Monte Carlo simulations with model potentials. Attention was also paid to the structure of single ion–water $Na^+(H_2O)_n$ and $I^-(H_2O)_n$ clusters, which are found to be non-spherically symmetric at room temperature. In agreement with earlier studies, $I^-(H_2O)_n$ clusters exhibit surface structures, with the "hydrophobic" iodide ion sitting at the surface of a water network, while room-temperature $Na^+(H_2O)_n$ clusters exhibit a solvation shell structure, where solvent molecules beyond the first solvation shell tend to accumulate on one side of the cluster instead of forming a spherical droplet. Both "contact" ion pairs (CIP) and solvent-separated ion pairs (SSIP) are found to have surface structures for the smaller clusters while both interior and surface structures may exist at room temperature for cluster size of 32. A remarkable feature of the ion pair cluster structural properties is that they are very much akin to those for individual ion–water clusters, especially for SSIPs, and some insight into the ion pair cluster structures can thus be gained from single ion–water cluster structures. We propose that the (small) extent of solvent–solvent hydrogen bonding and the magnitude of the (large) solvent dipole moments in the clusters can be used to illustrate the extent of the perturbation introduced by the ions or the ion pairs in the solvent environments. In contrast to the ion pair free energetics investigated in previous work, ion–water and salt-water cluster structural properties are rather insensitive to the choice of model potentials, whether one employs non-polarizable optimized potentials for liquid simulations (OPLS) such as TIP4P/OPLS or polarizable optimized potentials for cluster simulations. The structure of $NaI(H_2O)_n$ CIP and SSIP clusters have implications for the $NaI(H_2O)_n$ cluster photodissociation dynamics. The large solvent dipole moments obtained for $NaI(H_2O)_n$ clusters are indicative of increasingly larger local solvent dipoles in the clusters, which may then grow large enough to dipole-bind an electron upon cluster photoexcitation. Photoexcitation of the larger clusters might then proceed via a different route than it does for the small clusters and isolated NaI possibly involving a charge-transfer-to-solvent excited state akin to that of $I^-(H_2O)_n$ clusters. For the NaI photodissociation pathway, the surface structure of the small $NaI(H_2O)_n$ clusters may imply a slow change in the reaction dynamics with cluster size.

1. Introduction

As polar solvent molecules strongly affect the physical and chemical properties of species, increasing attention is being devoted to investigations of solute species in clusters of polar solvent

* Corresponding author. Fax: +1-970-491-3361.
E-mail address: bl@bibm.mfbl.colostate.edu (B.M. Ladanyi).

0301-0104/00/$ - see front matter
PII: S0301-0104(00)00106-3

molecules in order to understand the role of microsolvation in chemical reactions [1,2]. A number of experimental and theoretical studies focusing on the structure, thermodynamics and spectroscopy of such clusters have been reported, primarily for simple ion–solvent clusters [3–26], but also more recently for ion pairs or salts in clusters [27–32]. Studies of salts in water clusters may be relevant in environmental chemistry, atmospheric chemistry and cloud physics. For example, salts such as silver halides are typically used for cloud seeding and making artificial rain [33–35]. Hydrated sea-salt particles or water droplets containing sodium chloride or iodide are thought to be implicated in the heterogeneous chemistry that takes place in the marine boundary layer [36–42]. Thus, it is clear that deepening our understanding of the properties of salt-containing water clusters may bring some insight into such fields as cloud physics and atmospheric chemistry. In this article, we report a theoretical investigation of the structural properties of NaI salt in water clusters.

This article is the latest of a series which has centered on the photodissociation dynamics of NaI in solution [43] and in clusters [44]. The NaI system has long been a prototype system for the study of photodissociation dynamics involving curve crossing of covalent and ionic states [45–51], and as such, it serves as a paradigm system for our studies of solvation effects on the dynamics of chemical reactions. We have demonstrated in early work how a single water molecule influences the rate of non-adiabatic transitions between NaI electronic states, and how it affects the overall photodissociation dynamics of NaI [44]. The resulting simulated probe signal for $NaI(H_2O)$ photoionization was found to be in reasonable agreement with experiments carried out in connection with our theoretical work [52]. [1] We then addressed the stability of the ground state ion pair with respect to dissociation in the presence of polar solvent molecules [43], which is at the heart of the feasibility of the photodissociation experiments (one needs a stable ground state ion pair with an optically accessible excited state to start with).

[1] C. Jouvet and C. Dedonder-Lardeux, personal communication.

The stability of $NaI(H_2O)_n$ cluster ion pairs was investigated [53] by computing ion pair potentials of mean force and the resulting cluster ion pair equilibrium constants. The ion pair was found to be quite stable with respect to dissociation into free ions, even in very large clusters. Viewed in a larger perspective, the latter finding is in agreement with the results of NaCl simulations in supercritical water [54,55], experimentally derived equilibrium constants for NaI (or NaCl) ion pairs in low-polarity solvents [56,57], and recent free energy calculations of sulfuric acid ion pairs in large water mixture aerosols [30], and obviously contrasts with the situation in aqueous solutions under ambient conditions [58,59]. An analysis [53] of individual cluster ion and cluster ion pair solvation energies in terms of a simple cluster solvation dielectric model suggested that the stability of the ion pairs is in fact due to the slow convergence of the differential solvation free energy to the bulk limit, which in turn is due to the very slow convergence of cluster ion solvation energies with increasing cluster size [53]. This makes separated cluster ions thermodynamically very unlikely, and ions rather tend to exist as "contact" ion pairs (CIP) or solvent-separated ion pairs (SSIP). The latter SSIP species become thermodynamically predominant in the larger clusters [53].

Further, ab initio quantum chemistry calculations of model cluster excited states [53] suggested that the $NaI(H_2O)_n$ cluster CIP have optically accessible excited states akin to that of gas-phase NaI, hence making photodissociation experiments feasible, but that electronic transition oscillator strengths seem to significantly decrease for model SSIP, which become increasingly more likely with increasing cluster size. As a result, the larger (solvent-separated) cluster ion pairs may not be involved in photodissociation reactions via a mechanism akin to gas-phase NaI photodissociation, in agreement with recent experimental findings [53].

We now turn our attention to the structure of the NaI ion pairs in water clusters. A remarkable feature of the large halide ion–water clusters that has been observed experimentally [7,8] and theoretically [14,60–64] lies in their surface structure, which is attributed to the apparent "hydropho-

bicity'' of the large halide ions in water clusters: the ions tend not to adopt an interior solvated structure but rather sit at the surface of the water cluster. The latter can be simply explained in terms of the competition between solvent–solvent and ion–solvent potential interactions. Nothing of the sort has been reported or investigated in detail for other ions such as sodium, for which the ion–solvent interaction energy is so large that one readily assumes a fully solvated interior structure for the sodium–water clusters. If this is the case, the immediate question that comes to mind is whether a NaI ion pair sits at the surface of a water cluster or whether the sodium ion succeeds in dragging the large halide ion into the solvent network. We address this important issue in this article, after revisiting the structural properties of water clusters containing a single large halide ion such as iodide, and after investigating in detail the structure of the analog sodium–water clusters. We intend to show that much insight into the structure of ion pairs in water clusters can be gained from the knowledge of the structure of single ion–water clusters.

As in the previous work, we employ Monte Carlo simulations with model potentials to generate canonical ensembles of clusters at room temperature. There was a brief controversy [14] at one point whether non-polarizable model potentials such as TIP4P/OPLS [65] could account or not for the surface structure of large halide ion–water clusters. It has also been recently recognized that potentials primarily derived for liquid simulations may not be adequate for studies of clusters such as pure water clusters [66], and that new water model potentials may be needed to appropriately describe cluster properties. For this reason, we developed in our earlier work a simple polarizable water model along with ion–water potentials initially geared towards cluster simulations [53,67]. We will compare throughout this article ion–water and salt-water cluster structures predicted by simulations performed with both our model potentials and TIP4P/OPLS potentials, and we will pay attention to the sensitivity of the cluster structural properties to the choice of model potentials.

The outline of the remainder of this article is as follows: we first briefly review in Section 2 the cluster simulation procedure; we then present and discuss in Section 3 the structural properties of ion–water and salt-water clusters resulting from the simulations, and we discuss the possible implications of our findings for the $NaI(H_2O)_n$ cluster photodissociation dynamics. Concluding remarks follow in Section 5.

2. Interaction models and review of the simulation procedure

The simulation procedure employed in this work has been described in detail elsewhere [53], and we only outline its main features for completeness. Canonical ensembles of clusters at room temperature are generated as Markov chains by the random-walk Metropolis Monte Carlo method [68], where ions or ion pairs are held fixed in space, and new trial solvent configurations are generated by randomly translating one water molecule in each Cartesian direction and rotating it about its Euler angles. Since each random walk involves the six degrees of freedom of only one water molecule, the length of the Markov chains naturally increases with cluster size and we eventually store for structural analysis only sampled configurations for which all water molecules have changed positions. The ranges of displacements were typically chosen as 0.2 Å for translation, 20°, 0.2 and 20° for φ, $\cos\theta$ and ψ, respectively, where φ, θ and ψ are the standard Euler angles [68]. This prescription ensures an overall acceptance ratio of ~40% for new configurations. Attention was paid to water evaporation from the clusters – a possible event at room temperature – in order to sample a well-defined equilibrium ensemble of stable clusters of a given size. [2] This is achieved by adding a step

[2] It should be pointed out that computer simulations are performed for isolated clusters, whereas actual experimental measurements involve clusters of various sizes in thermodynamic equilibrium with the solvent vapor. The proper definition of the physical cluster has been a long-standing issue in investigations of nucleation and capillarity phenomena, but it is now generally agreed that thermodynamic properties computed for isolated clusters – the only practical approach at this point – give an adequate representation of the properties of clusters in equilibrium with the solvent vapor under realistic experimental conditions [69–72].

function in the configurational integral, so as not to take into account clusters that have undergone evaporation of one or more water molecules [18,73]. In practice, the conformational data is collected in chains of ≈10,000 configurations, and each chain containing clusters that have undergone water evaporation is excluded from the final conformational sampling. Each simulation entails 10^4 to 5×10^6 configurations of equilibration, depending on the size of the cluster, followed by an equivalent number of steps of conformational data collection. Finally, in order to attempt sampling of multiple possible local minima [74], the clusters are periodically heated and cooled with a smooth temperature schedule.

The intermolecular interactions in the cluster simulations are described by classical solvent–solvent and solute–solvent intermolecular potentials. Two different water potentials are employed in the simulations. The first water potential is the TIP4P/OPLS model [65], hereafter referred to as optimized potentials for liquid simulations (OPLS). The TIP4P model employs a rigid water molecule with experimental gas-phase geometry ($r_{OH} = 0.9572$ Å and $\theta_{H\text{–}O\text{–}H} = 104.52°$) and four interaction sites centered on the three nuclei and at a fourth point (M) on the bisector of the H–O–H angle, 0.15 Å from oxygen towards hydrogens. Hydrogens and the M site have point charges of $0.52e$ and $-1.04e$, respectively, while the oxygen, bearing no charge, carries a repulsion–dispersion term, i.e. a Lennard–Jones potential term with parameters $\varepsilon_{O\text{–}O} = 0.155$ kcal/mol and $\sigma_{O\text{–}O} = 3.154$Å. The solute–solvent OPLS parameters for Na^+–H_2O interactions ($\varepsilon_{O\text{–}Na^+} = 0.499$ kcal/mol and $\sigma_{O\text{–}Na^+} = 2.446$ Å) are taken from Jorgensen and co-workers [75], while the parameters for I^-–H_2O interactions ($\varepsilon_{O\text{–}I^-} = 0.225$ kcal/mol and $\sigma_{O\text{–}I^-} = 3.970$ Å) were derived so as to reproduce the experimental interaction energy and the calculated HF/3-21+G geometry of the ion–water complex [44,53], as was done in earlier work for other halide–water interactions [75].

Since there is some legitimate concern that water model potentials derived to reproduce bulk liquid properties may not be adequate for simulations of small clusters [66], we have developed a simple polarizable 5-site water model, together with optimized potentials for cluster simulations (OPCS) for the ion–water interactions. It turns out that our water model also provides a good description of bulk liquid water and details of the model properties are given elsewhere [67]. Briefly, our water model employs a rigid water molecule with experimental gas-phase geometry as for TIP4P, and consists of four charge sites, polarizable and repulsion–dispersion sites on the oxygen site, and H–H repulsion potential terms. The charge distribution is chosen so as to reproduce the experimental electric moments of water, including dipole and quadrupole moments: both of the hydrogens carry a charge $q_H = 0.569e$, while two M sites located at a distance of 0.342 Å from the oxygen on the bisector of the H–O–H angle, but off the water plane by an angle $\pm\theta_{H_2O\text{–}M} = 43.4°$, carry a charge $-q_H$. Non-additive many-body effects are accounted for via the polarizable site on the oxygen atom with polarizability chosen as the experimental isotropic value for the isolated water molecule ($\alpha_W = 1.45$ Å^3). The oxygen site carries a repulsion–dispersion term ($\varepsilon_{O\text{–}O} = 0.25$ kcal/mol; $\sigma_{O\text{–}O} = 3.20$ Å) as in the TIP4P model, and repulsion terms of the exponential form Ae^{-Br} ($A_{H\text{–}H} = 10^5$ kcal/mol; $B_{H\text{–}H} = 5.5$ Å^{-1}) are added between hydrogens. The intermolecular parameters for these potential terms are chosen to reproduce a wide range of experimental water dimer properties, such as binding energy, geometry, electrostatic properties and vibrational bending frequency [67]. The ion–water interactions are also modeled via Coulombic, polarization and Lennard-Jones potentials: the permanent charges on the ions are $\pm 1.0e$, the polarizabilities of the free ions are chosen as the gas-phase estimates of the ion polarizabilities ($\alpha_{Na^+} = 0.2$ Å^3; $\alpha_{I^-} = 7.0$ Å^3), and the Lennard-Jones terms are adjusted to fit experimental ion–water binding energies and ion–water complex ab initio MP2/6-31+G** minimum energy structure geometries [53].

The NaI ion pair potential model has been reported in earlier publications [43,44], to which the reader is referred for details. Briefly, a semiempirical quantum chemistry approach is employed to calculate the energy of Na^+I^- (and other va-

lence bond structures), including valence electron potential contributions, empirical core–core potentials and a classical polarization term to correct for the shortcomings of the valence-only minimum basis set approach of semiempirical quantum chemistry [44]. The ion polarizabilities are smoothly attenuated with decreasing internuclear separations, since the effective polarizability of the ions should naturally decline in the presence of other species. Energetics and dipole moments of the ground and first excited states of NaI, calculated via valence bond theory and our semiempirical quantum chemistry approach agree well both with those predicted by high level ab initio calculations [76] and with experimental values [45–50,77]. With the non-polarizable OPLS model, the ion pair polarization state is unaffected by the presence of solvent molecules and is that of gas-phase NaI, and the ions thus bear apparent fractional charges extracted from the NaI dipole moments. In contrast, with the fully polarizable OPCS model, the solvent molecules and the solute are allowed to polarize each other. To our knowledge, this work represents the first simulation of ion pairs in polar environments in which polar solvent molecules and solute can polarize each other, although this technique has been used extensively in ion–water simulations [60–64,78,79]. Even though simulations with both OPLS and OPCS models yield results with similar conclusions, there are some notable quantitative differences in the results which can be traced back to the explicit polarization term in OPCS [53]. For example, OPLS simulations predict an overwhelmingly more stable SSIP than the CIP for the $n = 16$–32 clusters, while the OPCS model predicts that the SSIP is only about 2–20 times more stable than the CIP. This illustrates the importance of including both solute–solvent and solvent–solvent many-body polarization terms in model potentials.

As mentioned earlier, the OPCS ion–water interaction parameters were fitted to reproduce $Na^+(H_2O)$ and $I^-(H_2O)$ cluster properties. Even though they were not included in the parameterization scheme, some properties of the small ion–water clusters (with two waters) and those of the small $NaI(H_2O)_n$ clusters ($n = 1$–2) predicted by the OPCS model compare favorably to their ab initio or experimental counterparts [53]. The small cluster properties are also reasonably well described by the OPLS model, but as expected, the agreement with ab initio and experimental properties is not as thorough. A notable advantage of the polarizable OPCS model, as noted above, lies in the better description of the charge distribution of the clusters, especially that of the water molecules. For example, the presence of a small charge-concentrated ion such as Na^+ strongly polarizes a nearby water molecule and enhances its dipole moment, a feature that is correctly accounted for by the OPCS model, but that cannot be properly described by the non-polarizable OPLS model.

3. Cluster structural properties

In this section, we present the structural properties of ion pairs in clusters. We start with an examination of the single ion clusters for reference, and then discuss CIP and solvent-bridged or SSIP in clusters. As we will see presently, the examination of the single ion clusters proves to be quite useful in rationalizing the observed ion pair cluster structures.

3.1. Single ion clusters

Fig. 1 shows representative structures of $Na^+(H_2O)_n$ and $I^-(H_2O)_n$ clusters from room-temperature ($T = 300$ K) simulations with both OPLS and OPCS, for cluster sizes of $n = 12$ and 20. As can be seen immediately from Fig. 1, the Na^+ ion tends to be solvated/surrounded by water molecules, while the I^- ion tends to remain at the water cluster surface. The latter feature, observed for the larger single halide ion–water clusters [7,8,60–64], is due to the fact that, in contrast to the case of Na^+, the stabilization energy gained by solvating I^- does not compensate the (free) energy loss associated with disrupting/breaking the hydrogen-bonded water network [80]; in other words, the solvent–solvent interactions seem to prevail over the solute–solvent interactions in

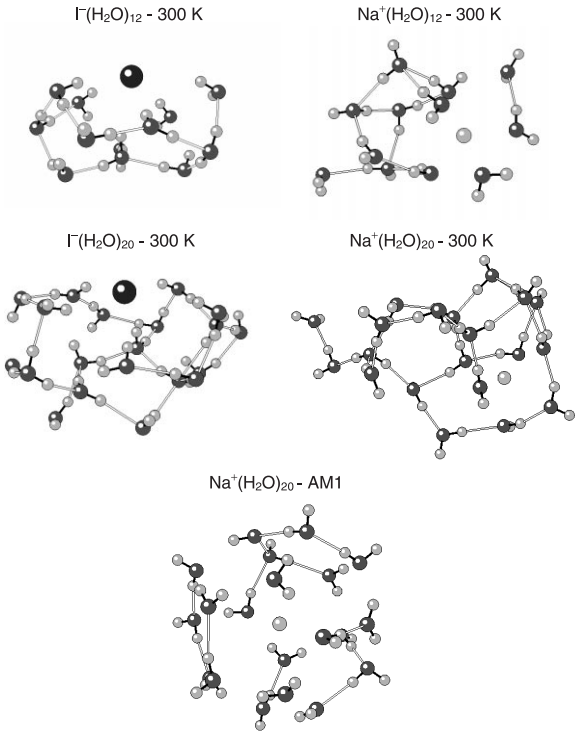

Fig. 1. Typical $Na^+(H_2O)_n$ and $I^-(H_2O)_n$ cluster structures at 300 K, $n = 12$ and 20. The symmetrical cage-like structure of $Na^+(H_2O)_{20}$ obtained with the semiempirical AM1 method [83] is also shown.

determining the structure of the large halide ion–water clusters.

Radial intermolecular ion–O or ion–H and O–H probability distributions for $Na^+(H_2O)_n$ and $I^-(H_2O)_n$ clusters are shown in Figs. 2 and 3, respectively, for both OPLS and OPCS. It should be noted that the latter distributions differ from the radial distribution functions $g(r)$ used in liquid structure theory by a factor $4\pi r^2$ and actually represent relative probabilities. These probabilities are properly normalized so that the integral distributions equal the number of solvent molecules present in the cluster; for example, the ion–O or ion–H probability distribution represent the derivative of the distance-dependent ion–solvent coordination number $N_{\mathrm{coord}}(r)$.

$$P(r) = \frac{\mathrm{d}N_{\mathrm{coord}}(r)}{\mathrm{d}r} = n\frac{4\pi r^2 g(r)}{\int_0^\infty 4\pi r^2 g(r)\,\mathrm{d}r}.$$

This definition ensures that $\int_0^\infty P(r)\,\mathrm{d}r = n$, and that comparisons can be made between distributions obtained for different ions, model potentials and cluster sizes. Note that in clusters $g(r)$ vanishes for distances r larger than the cluster dimensions.

Inspection of Figs. 2 and 3 immediately reveals that the sodium ion in $Na^+(H_2O)_n$ clusters exhibits a solvation shell structure, identified by sharp peaks in the probability distribution function, which is absent or not as pronounced for iodide in clusters of the same size. From the integral distributions, one notes that the first solvation shell for the sodium ion is complete with five to six water molecules, while the iodide ion seems to be directly hydrogen-bonded to about only four water molecules, consistent with a cluster surface structure, where only a few solvent molecules are in contact with the ion. The intermolecular O–H probability distributions for the ion–water clusters contrast with those of liquid water (not shown here, but they can be obtained from radial distribution functions given in Ref. [81]) in that they do not exhibit two clear peaks, such as for bulk water. The intermolecular O–H probability distributions rather have a long tail that is representative of structureless solvent; the extent of solvent–solvent hydrogen bonding is also rather small for both ion–water clusters and does not seem to increase significantly with cluster size. Further, the integral number of hydrogen bonds per water molecule is close to 1, which illustrates how the presence of the ion perturbs the hydrogen-bonded water network, even for iodide-water clusters. The latter number could serve as a measure of the perturbation introduced by ions, or more generally, solutes in water clusters. Thus, it will be of interest to compare the intermolecular O–H probability distributions and the integral number of hydrogen bonds per water molecule of the ion-containing water clusters to those of pure solvent clusters [67].

In order to make a more systematic analysis of the ion–water cluster structures, convenient water position coordinates can be defined [82] as the distance R_{cm} between the ion and the solvent subcluster center of mass, and the angle θ between the solvent molecule, the ion and the solvent subcluster center of mass, as schematically depicted in

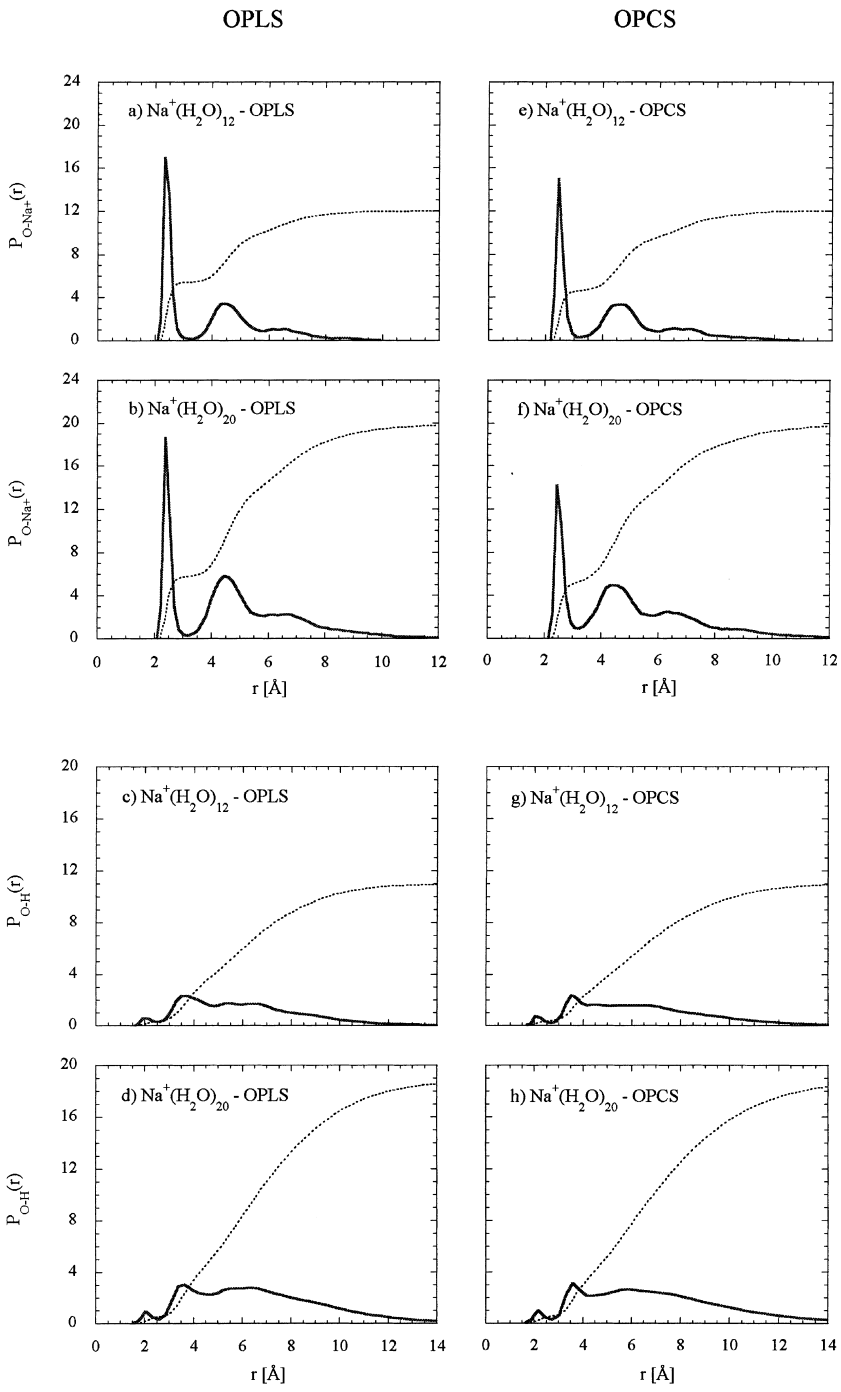

Fig. 2. $Na^+(H_2O)_n$ cluster structural properties. Radial intermolecular ion–O and O–H relative probabilities for $n = 12$ and 20 with both OPLS and OPCS models. Also shown are the integral probabilities, i.e. solvent running coordination numbers, $N_{\text{coord}}(r)$, as dotted lines. The distributions are evaluated from ensembles containing ≈5000 configurations generated at 300 K.

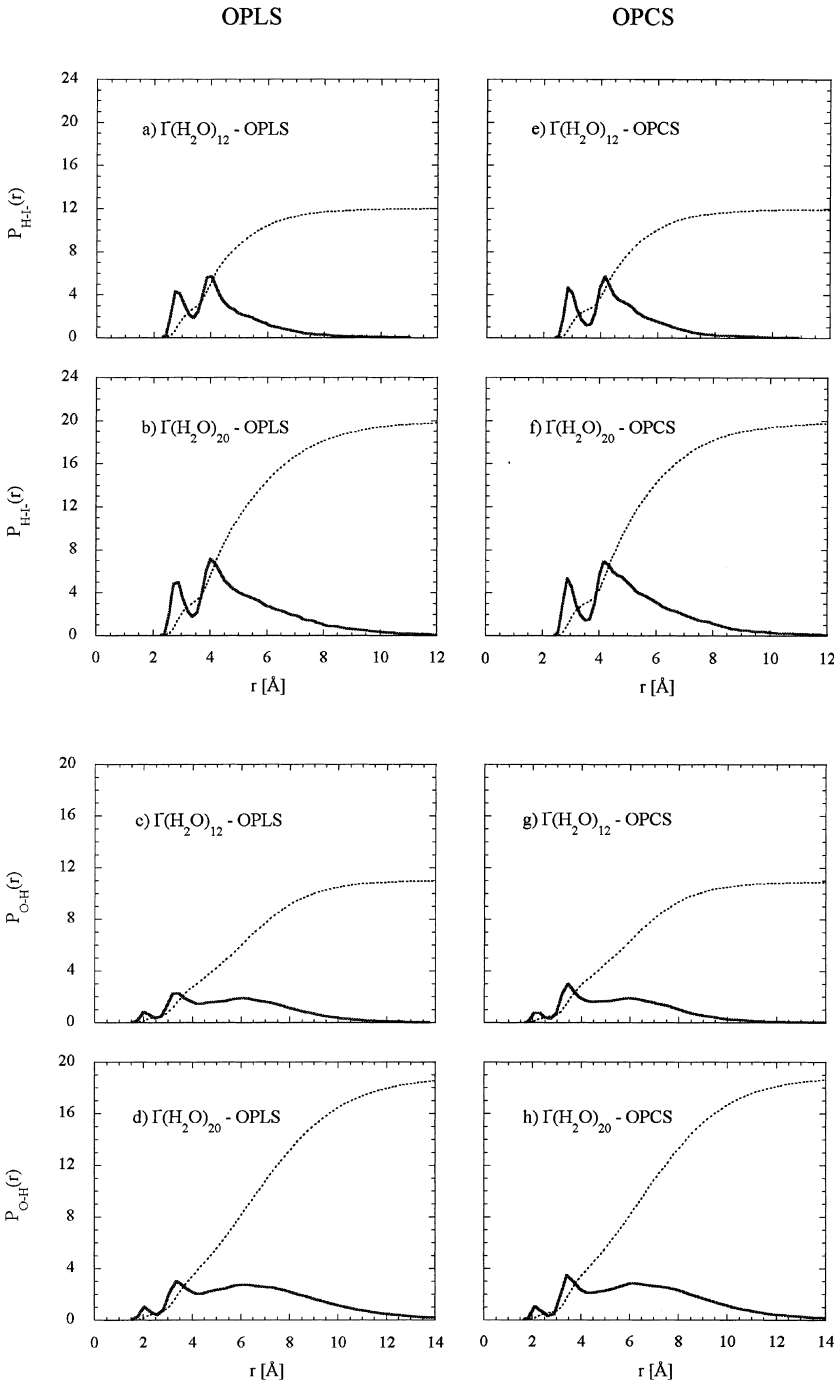

Fig. 3. $I^-(H_2O)_n$ cluster structural properties. Radial intermolecular ion–H and O–H relative probabilities for $n = 12$ and 20 with both OPLS and OPCS models. Also shown are the integral probabilities, i.e. solvent running coordination numbers, $N_{\text{coord}}(r)$, as dotted lines. The distributions are evaluated from ensembles containing ≈5000 configurations generated at 300 K.

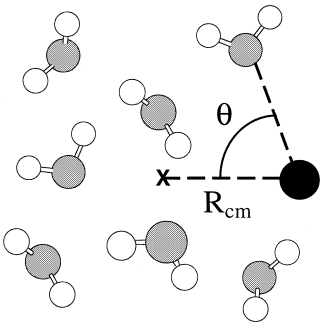

Fig. 4. Schematic representation of the water molecule position coordinates in ion–water clusters. R_{cm} is the distance between the ion and the solvent sub-cluster center of mass, while θ is the angle between the solvent molecule, the ion and the solvent sub-cluster center of mass.

Fig. 4. R_{cm} and θ distribution functions are shown in Figs. 5 and 6 for $Na^+(H_2O)_n$ and $I^-(H_2O)_n$ clusters, respectively, for both OPLS and OPCS. From the R_{cm} and θ distributions, it is obvious that the $I^-(H_2O)_n$ clusters exhibit more surface-like structures than do the $Na^+(H_2O)_n$ clusters, with the solvent center-of-mass clearly further away from the ion and with many fewer water molecules on average on the other side of the ion. However, the $Na^+(H_2O)_n$ clusters are not spherically symmetric at room temperature and only one solvation shell is complete, even for $n = 20$. The latter size was chosen because it corresponds to a "magic" number for which $Na^+(H_2O)_n$ clusters can adopt a spherically symmetric cage-like structure reminiscent of a Buckyball or clathrates [23]. Such a cage-like $Na^+(H_2O)_{20}$ cluster structure, as optimized with the AM1 semiempirical quantum chemistry method [83], is shown in Fig. 1.

The non-spherical feature of the ion–water clusters can be further illustrated by the distributions of the cluster moments of inertia, as listed in Tables 1 and 2 for $Na^+(H_2O)_n$ and $I^-(H_2O)_n$, respectively. From the difference in magnitude of the various principal moments of inertia, one can immediately see that these clusters are not spherically symmetric at room temperature, while the cage-like $Na^+(H_2O)_{20}$ cluster structure is almost perfectly spherically symmetric. For the $Na^+(H_2O)_n$ clusters, however, the relative magnitudes of the principal moments of inertia for the first solvation shell (whose boundary is identified by the first minimum in the ion–water radial distribution functions in Fig. 3) are not as spread out as for the whole cluster, indicating that mainly the molecules beyond the first solvation shell are responsible for the non-spherical cluster structures. As expected, the moments of inertia of the clusters are more spread out for $I^-(H_2O)_n$ than for $Na^+(H_2O)_n$.

The reason for the sodium–water cluster structures observed is evidently that, in order to minimize the cluster free energy, water molecules naturally surround the sodium ion, but once a solvation shell is complete, the strength of the solute–solvent interactions in the next solvation shell may be weaker than the solvent–solvent interactions, so that the solvent molecules accumulate on one side of the cluster instead of forming a spherical droplet. (At large enough cluster sizes, entropy and long-range polarization effects may finally drive the ion towards the center of the cluster.) Thus, for smaller cluster sizes, the sodium ion–water cluster is not spherical on average at room temperature, and the second solvation shell cannot be completed for the sodium ion until cluster sizes of 20 or more are reached. At low temperatures, the second solvation shell may be complete for cluster size 20 as the $Na^+(H_2O)_{20}$ clusters may exhibit a well-organized cage-like structure shown in Fig. 1 [23], but at room temperature, it is clear that $Na^+(H_2O)_{20}$ clusters do not possess spherical symmetry (even though the simulations were initiated with the spherical cage-like structure).

As expected for a non-spherically symmetric species, the net total dipole moments of the clusters listed in Tables 1 and 2 are significant, and they are larger for $I^-(H_2O)_n$ than for $Na^+(H_2O)_n$. We note that the dipole moment of a charged species is not independent of the choice of origin, so we choose the position of the ion as origin, so that the calculated dipole moment is that "felt" by the ion due to the solvent or is just the solvent subcluster net dipole moment. The magnitude of the solvent dipole moments is quite large for ion–water clusters. It is also quite remarkable that even cage-like ion–water cluster structures (or the well-defined first solvation shell of $Na^+(H_2O)_n$ clusters)

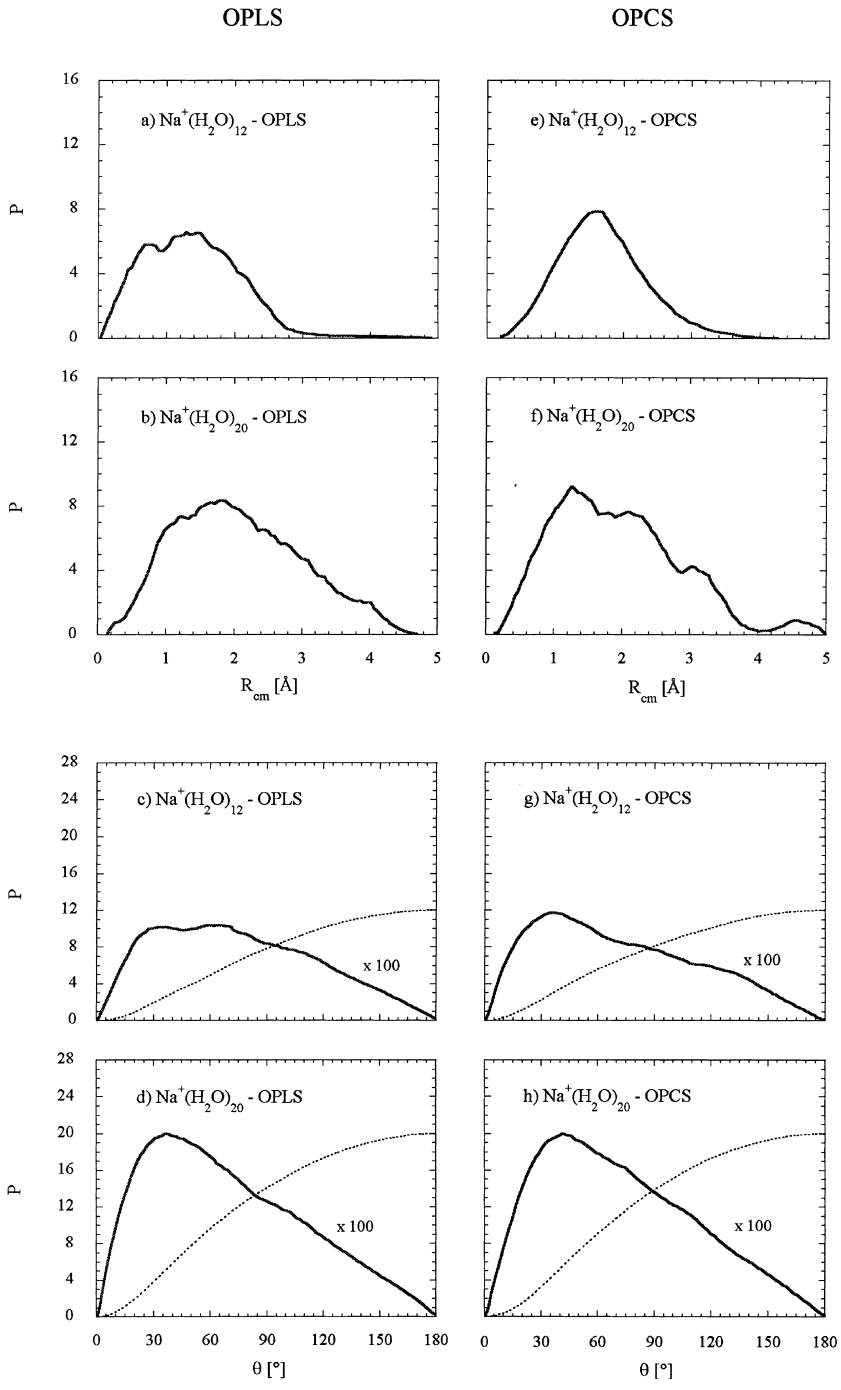

Fig. 5. $Na^+(H_2O)_n$ cluster structural properties. Distributions of the R_{cm} and θ coordinates of the water molecules for $n = 12$ and 20 with both OPLS and OPCS models. Also shown are the integral probabilities in dotted lines. The distributions are evaluated from ensembles containing ≈5000 configurations generated at 300 K.

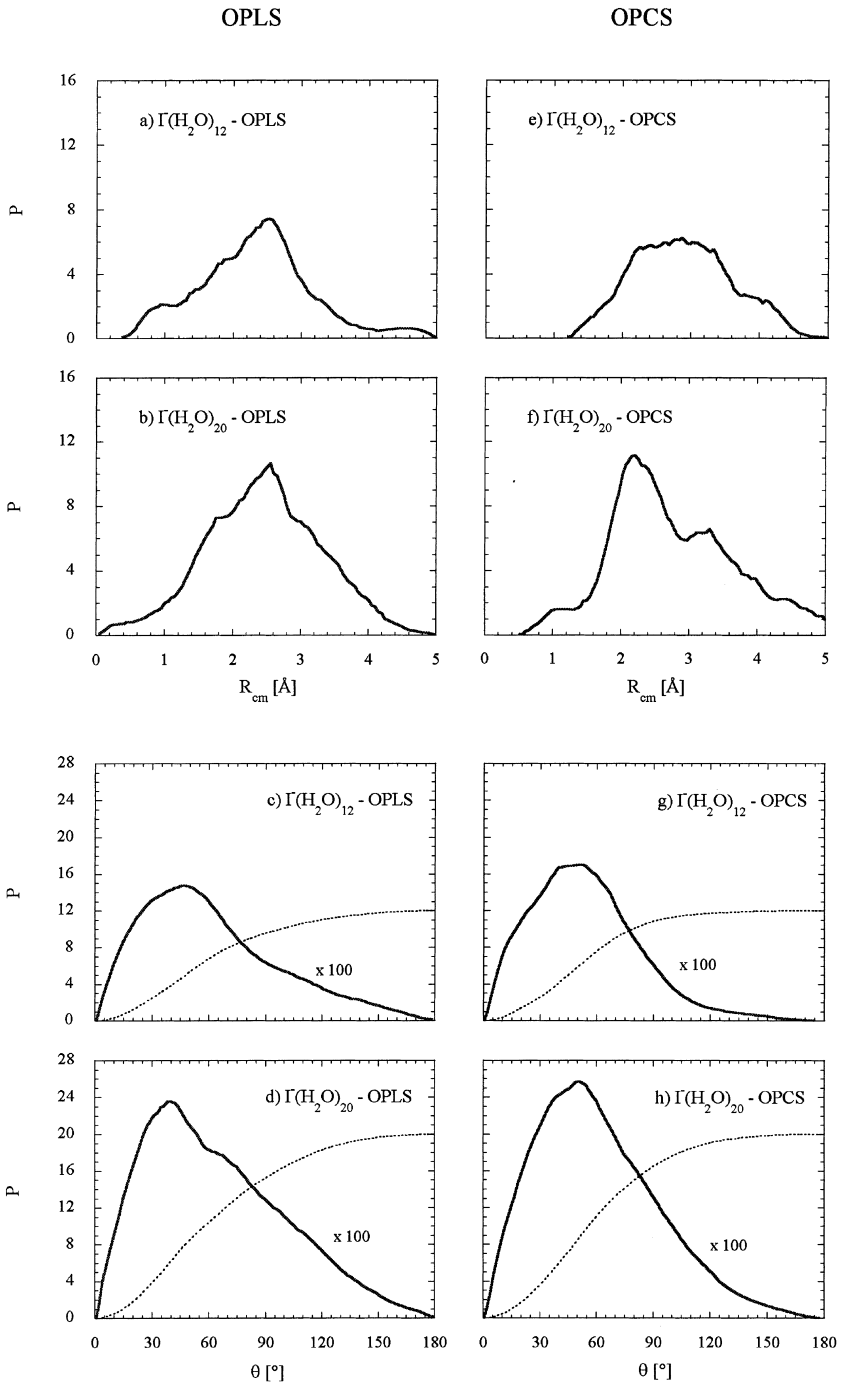

Fig. 6. $I^-(H_2O)_n$ cluster structural properties. Distributions of the R_{cm} and θ coordinates of the water molecules for $n = 12$ and 20 with both OPLS and OPCS models. Also shown are the integral probabilities in dotted lines. The distributions are evaluated from ensembles containing ≈5000 configurations generated at 300 K.

Table 1
Structural properties of $Na^+(H_2O)_n$ clusters[a]

	$\langle R_{cm}\rangle$[b]	$\langle\theta\rangle$[c]		$\langle I\rangle$[d]		$\langle\mu_T\rangle$[e]
n = 12 − OPLS						
	1.31 ± 0.63	73 ± 40	1340 ± 270	2760 ± 840	3340 ± 810	7.1 ± 3.1
First solvation shell	0.29 ± 0.14	83 ± 38	330 ± 51	380 ± 59	450 ± 48	2.9 ± 1.2
n = 12 − OPCS						
	1.64 ± 0.57	70 ± 42	1440 ± 360	3250 ± 670	3820 ± 715	7.6 ± 2.8
First solvation shell	0.34 ± 0.15	80 ± 37	270 ± 53	340 ± 55	410 ± 63	2.9 ± 1.2
n = 20 − OPLS						
	2.04 ± 0.90	68 ± 40	3380 ± 670	6420 ± 2020	7580 ± 2200	10.6 ± 4.4
First solvation shell	0.25 ± 0.12	83 ± 38	370 ± 47	410 ± 52	460 ± 47	3.4 ± 1.4
n = 20 − OPCS						
	1.88 ± 0.89	70 ± 39	3930 ± 1076	6700 ± 1830	8480 ± 2380	10.4 ± 4.6
First solvation shell	0.39 ± 0.17	81 ± 38	330 ± 74	400 ± 81	470 ± 81	3.8 ± 1.6
n = 20 − cage-like structure (*AM1*)						
	0.1	89 ± 39	4440	4510	4670	3.9

[a] The listed values are average and standard deviation of each structural property for ensembles of ≈5000 configurations generated at 300 K (except for the cage-like structure – see text).
[b] Average distance (in Å) between the ion and the solvent cluster center of mass, as depicted in Fig. 4.
[c] Average angle (in degrees) between the individual water molecules, the ion and the solvent center of mass, as depicted in Fig. 4.
[d] Principal moments of inertia in amu Å^2.
[e] Total cluster dipole moment in D calculated with the ion position taken as origin.

Table 2
Structural properties of $I^-(H_2O)_n$ clusters[a]

	$\langle R_{cm}\rangle$[b]	$\langle\theta\rangle$[c]		$\langle I\rangle$[d]		$\langle\mu_T\rangle$[e]
n = 12 − OPLS	2.24 ± 0.73	60 ± 35	1600 ± 400	2840 ± 760	3440 ± 940	8.5 ± 3.3
n = 12 − OPCS	2.86 ± 0.70	52 ± 28	1640 ± 380	2670 ± 836	3380 ± 1190	8.0 ± 3.2
n = 20 − OPLS	2.43 ± 0.83	63 ± 36	3650 ± 880	7100 ± 2100	8270 ± 2250	11.1 ± 4.2
n = 20 − OPCS	2.73 ± 0.90	59 ± 32	3700 ± 730	6790 ± 1730	7990 ± 1820	10.1 ± 4.4

[a] The listed values are average and standard deviation of each structural property for ensembles of ≈5000 configurations generated at 300 K.
[b] Average distance (in Å) between the ion and the solvent cluster center of mass, as depicted in Fig. 4.
[c] Average angle (in degrees) between the individual water molecules, the ion and the solvent center of mass, as depicted in Fig. 4.
[d] Principal moments of inertia in amu Å^2.
[e] Total cluster dipole moment in D calculated with the ion position taken as origin.

have significant non-zero solvent dipole moments, which are due to the ion-induced orientation of the water molecules. For the purpose of measuring the extent of the perturbation introduced by various ions (or other solute species), it will be of interest to compare in greater detail the net solvent dipole moments of pure solvent clusters to those of ion-containing species [67].

Finally, inspection of the R_{cm} and θ values in Tables 1 and 2 confirms that the $I^-(H_2O)_n$ clusters exhibit a much more pronounced surface character than the $Na^+(H_2O)_n$ clusters, as already mentioned, but also this feature of the large halide ion–water clusters seems slightly more prominent for OPCS. It is however remarkable that both OPLS and OPCS predict very similar structural properties (as can be seen from Figs. 2, 3, 5 and 6, and Tables 1 and 2), given the fact that they predict quantitatively very different ion pair energetics and free energetics [53]. We note in passing that similar findings are quite common in quantum chemistry calculations, where molecular geometries are not as sensitive to the choice of level of electronic structure theory and basis set as energetics are,

and, e.g., low level model chemistries often appropriately describe molecular geometries while predicting poor energetics. In conclusion, structural properties of ion–water clusters seem to be fairly robust vis a vis choice of model potentials while their energetics are much more sensitive to the choice of model potentials employed in simulations. Let us now turn our attention on ion pairs in water clusters.

3.2. Ion pair clusters

Fig. 7 shows representative structures of CIP $NaI(H_2O)_n$ clusters from room-temperature ($T = 300$ K) simulations, for cluster sizes of $n = 16$ and 32. The OPLS and OPCS ion pair–water cluster structures displayed were obtained for NaI internuclear separations of $r = 2.8$ Å and $r = 3.0$ Å, respectively, which are close to separations for which the potentials of mean force exhibit a first minimum for both cluster sizes [53]. These clusters are thus representative of CIP. A striking feature of the representative cluster structures is the surface character of the NaI solute in the small water clusters, i.e. the iodide ion tends to "sit" at the surface of the cluster, dragging the sodium ion along towards the surface of the cluster. This can be traced back to the "hydrophobicity" of the iodide ion, observed in other cluster studies [7,8, 60–64,82] and discussed earlier.

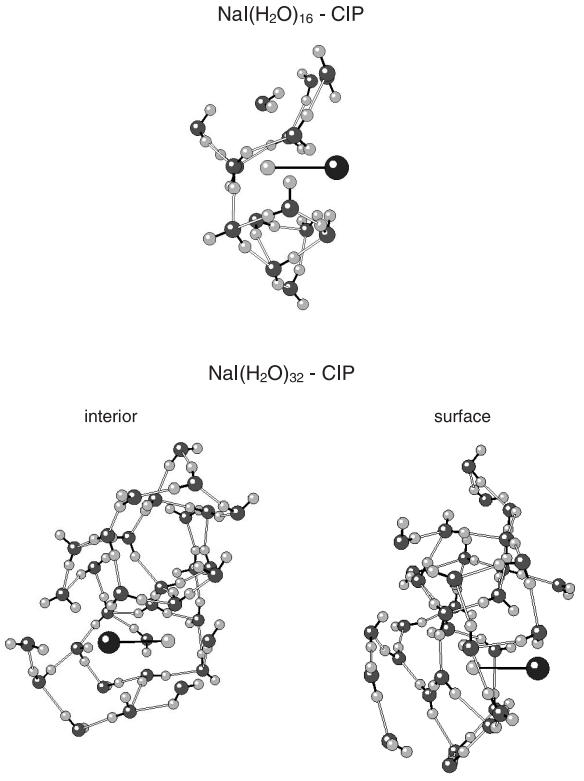

Fig. 7. Typical $NaI(H_2O)_n$ CIP cluster structures at 300 K.

In order to make a more systematic analysis of the $NaI(H_2O)_n$ cluster structures, we define a water position coordinate as the angle Θ between NaI and the vector joining the water oxygen atom to the geometric center of NaI, as schematically represented in Fig. 8. Small Θ angles are representative of waters on the sodium side, while large Θ angles are representative of waters on the iodide side of the cluster. The distributions of the Θ angles are displayed in Fig. 9 for CIP clusters of size $n = 16$ and 32, along with the ion pair–solvent cluster center of mass R_{cm} distributions, which also illustrate the surface character of the small CIP cluster structures. Obviously, for an ideally spherical cluster, the waters would have a uniform probability of being located at a given distance from the NaI solute geometric center in space, resulting in a probability of finding a water at an angle Θ proportional to $\sin\Theta$ (the angular part of

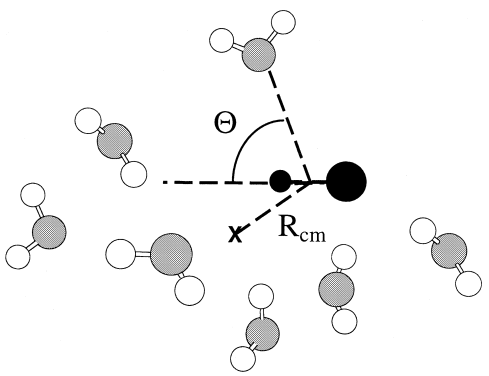

Fig. 8. Schematic representation of the water molecule position coordinates in ion pair–water clusters. Θ is the angle between NaI and the vector joining the water oxygen atom to the geometric center of NaI. Small Θ angles are representative of waters on the sodium side, while large Θ angles are representative of waters in the iodide side of the cluster.

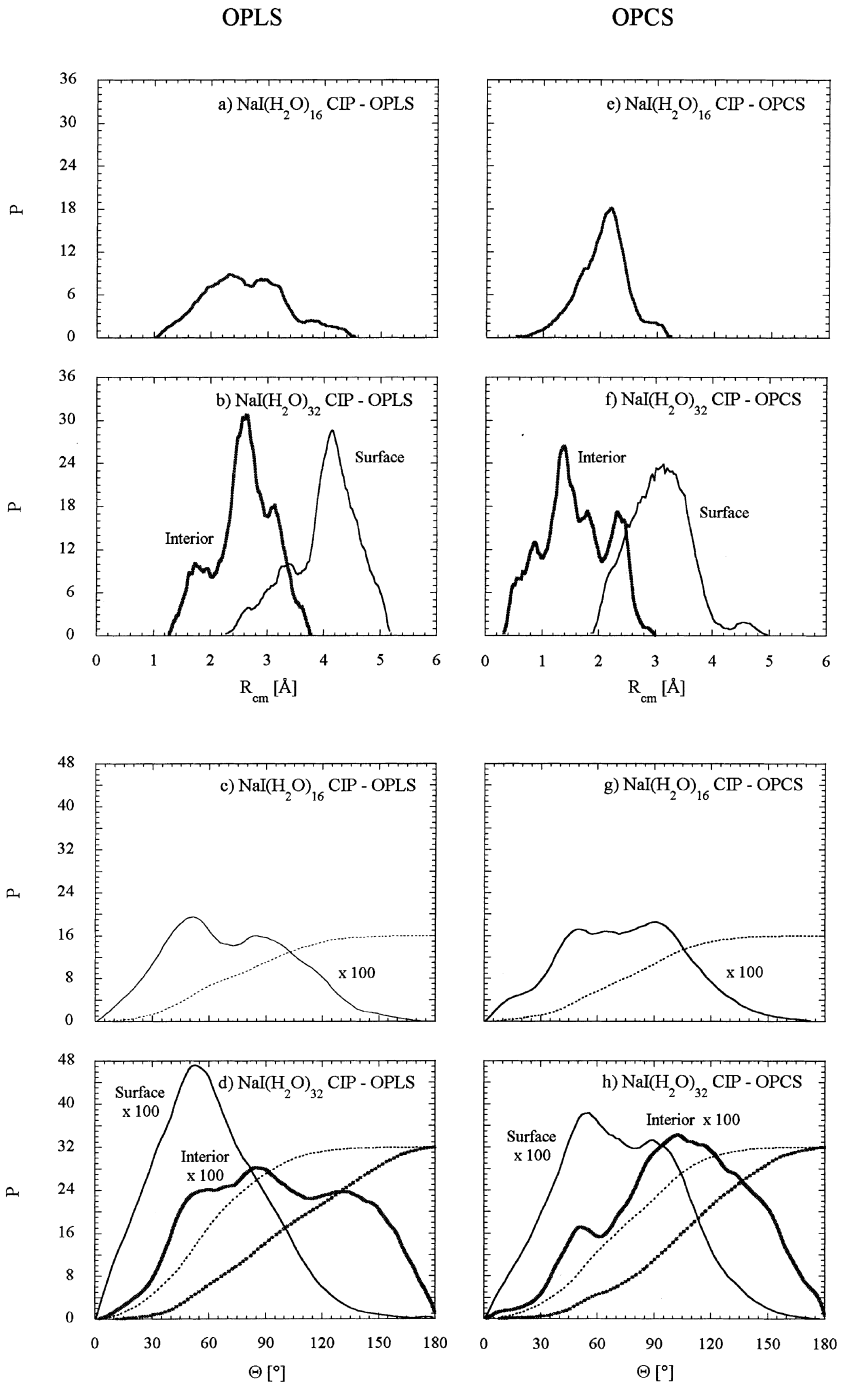

Fig. 9. $NaI(H_2O)_n$ CIP cluster structural properties. Distributions of the R_{cm} and Θ coordinates of the water molecules for $n = 16$ and 32 with both OPLS and OPCS models. Also shown are the integral probabilities in dotted lines. The distributions are evaluated from ensembles containing ≈5000 configurations generated at 300 K.

Table 3
Structural properties of contact ion pair $NaI(H_2O)_n$ clusters[a]

	$\langle R_{cm}\rangle$[b]	$\langle\Theta\rangle$[c]	$\langle I\rangle$[d]			$\langle\mu_T\rangle$[e]
n = 16 – OPLS	2.60 ± 0.70	71 ± 31	2550 ± 690	4710 ± 1660	5610 ± 1990	9.3 ± 2.9
n = 16 – OPCS	2.03 ± 0.43	73 ± 30	2740 ± 830	4780 ± 1830	5700 ± 2120	12.4 ± 2.9
n = 32 – OPLS						
Interior	2.58 ± 0.51	97 ± 38	7790 ± 920	11700 ± 1350	14100 ± 1280	11.5 ± 3.7
Surface	3.99 ± 0.59	59 ± 28	7180 ± 720	11000 ± 1340	12300 ± 1320	9.9 ± 3.7
n = 32 – OPCS						
Interior	1.55 ± 0.57	102 ± 35	8430 ± 700	11300 ± 1000	12900 ± 1210	15.2 ± 3.6
Surface	3.05 ± 0.52	70 ± 30	7900 ± 940	11000 ± 1230	13100 ± 1280	12.3 ± 3.5

[a] The listed values are average and standard deviation of each structural property for ensembles of ≈5000 configurations generated at 300 K.
[b] Average distance (in Å) between the ion and the solvent cluster center of mass, as depicted in Fig. 8.
[c] Average angular position (in degrees) of the water molecules, as depicted in Fig. 8.
[d] Principal moments of inertia in amu Å^2.
[e] Total cluster dipole moment in D.

the elementary volume element in polar coordinates). Thus, for an ideally spherical cluster, Θ angles of 90° are most probable, while angles of 0° and 180° are less likely, and the average Θ value is 90°. It is obvious from Fig. 9 that the water angular distributions for clusters of size 16 do not exhibit a $\sin\Theta$-like dependence, and thus, the clusters are not spherically symmetric. The average angular positions of the waters listed in Table 3 indicate that both models yield similar structural properties for small clusters, and that the waters are predominantly located on the sodium side in surface clusters. Also, the deviation from the average value of 90° for a spherical cluster decreases with cluster size increase, indicating that the larger clusters possess an increasingly spherical symmetry, and there seems to be a transition from surface to interior clusters by the time size 32 is reached, as addressed now.

For $NaI(H_2O)_{32}$ clusters, both interior and surface structures exist at room temperature, as shown in Fig. 7, and they are apparently separated by rather large effective free energy barriers: simulations initiated with one of the structures mainly sample the phase space of that particular structure, and despite heating of the clusters up to 900 K (at which temperature, water evaporation occurs quite often and rapidly) and cooling down periodically to 300 K in an effort to sample as many local minima as possible, the other structural configurations are rarely accessed in the course of the Monte Carlo simulation. Both model potentials predict at least two local minimum energy structures that we could identify for $NaI(H_2O)_{32}$ clusters, interior and surface structures, which lie within a few kcal/mol in energy with OPLS and are almost isoenergetic for OPCS, and thus, both structural states could be nearly equally populated at room temperature. As just mentioned, simulations initiated around a given stable structure mainly sample that structure (even after heating/cooling of the clusters), so which structures are actually more likely to occur in experiments may just depend on how clusters are prepared, as there are large effective free energy barriers for cluster isomerization/interconversion. In the following, we present results for clearly distinct ensembles of both sets of structures obtained separately from simulations without heating/cooling of the clusters. The free energetics of interior vs. surface solvation for these ion pairs and the resulting relative equilibrium populations of interior and surface cluster structures are under investigation and will be reported elsewhere [84]. We note in passing that the potentials of mean force for the $NaI(H_2O)_{32}$ cluster ion pairs obtained in previous work [53] are the same, within statistical uncertainties, whether one samples distinct ensembles of surface or interior structures.

The two distinct room-temperature ensembles of $NaI(H_2O)_{32}$ cluster structures just identified obviously have very different features. As can be

seen from Table 3, interior structures are characterized by smaller average R_{cm} values and average Θ angles closer to 90°, while surface structures possess larger average R_{cm} values and average Θ angles smaller than 90°. It is remarkable that the interior structures have Θ angular distributions biased towards larger angles, and consequently average Θ values larger than 90°. This can be traced back to the fact that only simulations started with a large excess of water molecules around iodide lead to interior structures; those started with an equal amount of water molecules on each ion invariably lead to surface structures. As a result, only interior structures with an excess solvent water molecules around the iodide ion exist as such. The probability distribution functions for both interior and surface structures, displayed in Fig. 10, show that there is obviously a bit less solvent structure around the iodide ion for surface structures than for interior structures. Finally, we note from inspection of the moments of inertia in Table 3 that both classes of structures seem to have similar cylindrical symmetry.

The probability distribution functions displayed in Fig. 10 for CIPs are strikingly similar to their counterparts for single ion–water clusters. The long tail of the ion pair–water clusters probability distribution functions obviously differs from that for the single ion–water clusters past the first peak, but for the most part, the local solvent environment around the sodium ion in the first solvation shell and around the iodide ion in the CIP clusters is very similar to that for the single ions. Again, we note that the solvent–solvent hydrogen bonding is quite similar for ion pair–water clusters, whether interior or surface structures, and for ion–water clusters. We thus propose to rationalize the observed CIP cluster structures, based on the structural properties of single ion clusters. As mentioned earlier, the surface character of the small $NaI(H_2O)_n$ clusters naturally arises from a competition between the halide "hydrophobic" tendency to be on the surface of the cluster [7,8,60–64,82] and the sodium tendency to be solvated. It is clear that the halide ion hydrophobicity prevails in determining the most thermodynamically stable surface cluster structures, even though simple energetic arguments would predict the opposite as the magnitude of the binding energy of water to sodium is more than twice that of water to iodide.

We now attempt to utilize the results of Section 3.1 to gain some understanding of the $NaI(H_2O)_n$ cluster structures. $Na^+(H_2O)_n$ clusters grow in a non-symmetrical fashion and only the ion first solvation shell is complete for cluster sizes up to 20 or more, so that, for the latter ion–water cluster sizes, there is always one side of the ion with only one water molecule nearby. Removal of that one water molecule from the first solvation shell and replacing it by the iodide ion may result in a stable structure, where the sodium ion–water structure is perturbed in a minimal fashion. Of course, structures obtained by this simplistic substitution of a water by iodide are not totally representative of the actual $NaI(H_2O)_n$ cluster structures, as the iodide ion is also solvated by more water molecules; nonetheless, at a qualitative level, structural features of the sodium ion–water clusters may explain why the iodide ion is able to drag the sodium ion towards the surface of the cluster, up to reasonable ion pair–water cluster sizes. For cluster sizes of 32 or more water molecules, this simplistic explanation starts to break down as a second solvation shell would start closing around the sodium ion, and the simple substitution scheme would not hold anymore. This coincides with the emergence of possible interior cluster structures, which are only possible when a large number of water molecules is floating on the iodide side of the ion pair, obviously because iodide is the hard one to solvate.

We now turn our attention to the structural properties of SSIPs. Fig. 11 shows representative structures of SSIP $NaI(H_2O)_n$ clusters from room-temperature ($T = 300$ K) simulations with both OPLS and OPCS. A striking feature of the SSIP structures is that they have a more pronounced surface character than CIPs. As a matter of fact, OPLS predict only surface $NaI(H_2O)_{32}$ SSIP structures, whereas both interior and surface structures exist at room temperature for CIPs of the same cluster size. $NaI(H_2O)_{32}$ SSIPs tend to have similar cylindrical symmetry and similar Θ angular distributions as their analog CIPs, as can be seen from Table 4 and Fig. 12, but they exhibit quite different R_{cm} distributions. The latter seem

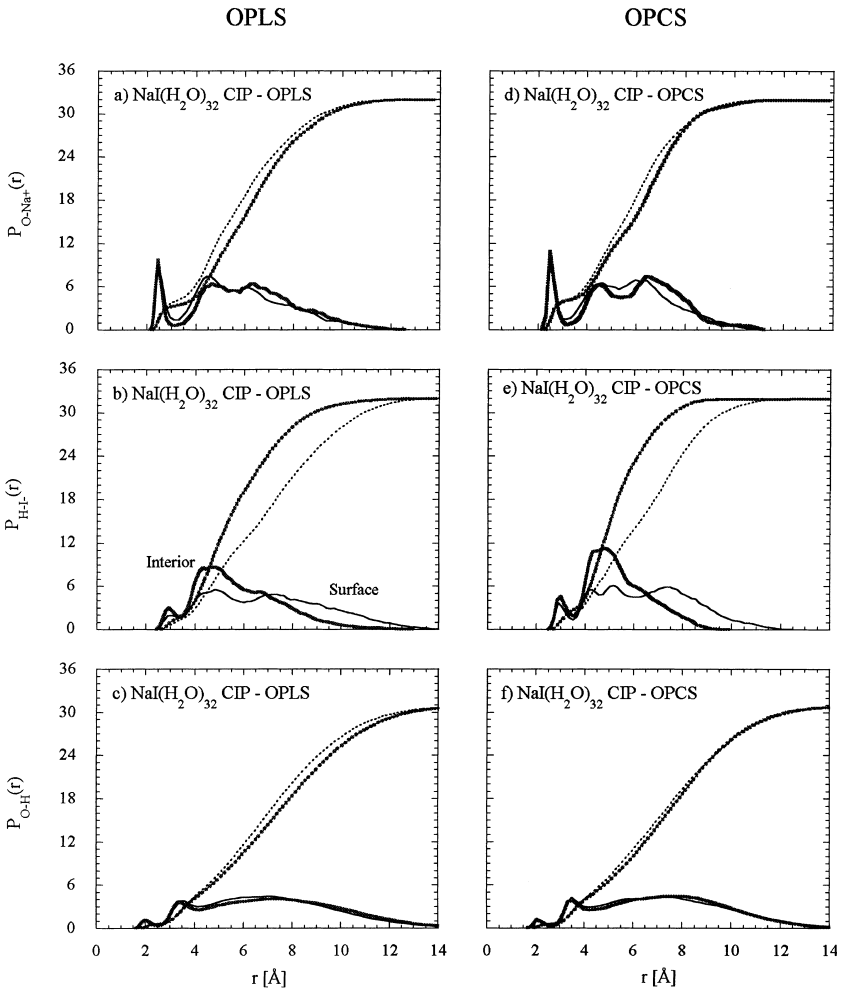

Fig. 10. $NaI(H_2O)_{32}$ CIP cluster radial O–Na^+, H–I^- and O–H probability distributions with both OPLS and OPCS models. Also shown are the integral probabilities in dotted lines.

actually counter-intuitive as interior structures are predicted to have larger R_{cm} values than surface structures by OPCS. This is simply due to a large excess of water molecules on the iodide side for the interior SSIPs (very much like for interior CIPs), and as a result, the solvent center of mass is displaced further out from the center of the ion pair (and the effect is larger as the ions are further apart). For these reasons, the R_{cm} coordinate does not appear to be as useful for characterizing interior and surface structures as it is for ion–water clusters, but the Θ angular distributions however, can still fulfill that role.

The $NaI(H_2O)_n$ SSIP probability distributions displayed in Fig. 13 are very much like those for the single ion–water clusters, except of course for the long tail of the SSIP probability distributions which indicate a lower degree of solvent structure for distant water molecules, due to the influence of the other ion. The similarity between the ion pair–water and ion–water cluster probability distributions is, not surprisingly, even more pronounced for SSIPs than for CIPs, and clearly, one could envision building SSIP cluster structures by placing a $Na^+(H_2O)_n$ cluster with one complete solvation shell (and not necessarily spherically

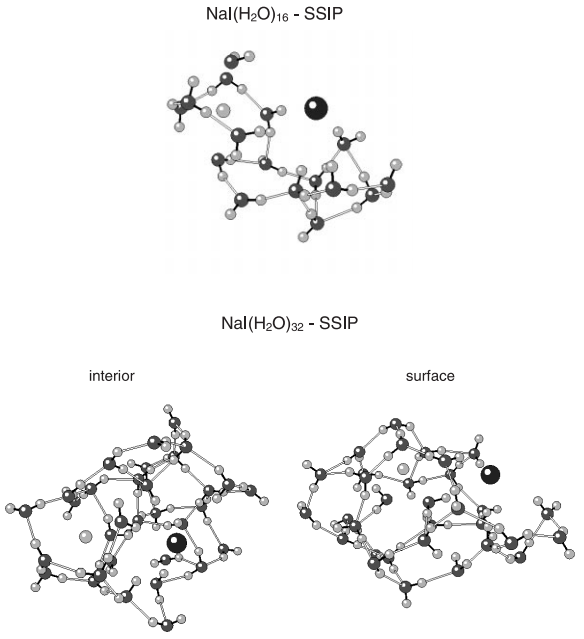

Fig. 11. Typical $NaI(H_2O)_n$ SSIP cluster structures at 300 K.

symmetric) together with a surface $I^-(H_2O)_n$ cluster.

Finally, we note that the net solvent dipole moments listed in Tables 3 and 4 (now independent of origin for neutral clusters) are also quite significant for all ion–pair cluster structures, and even more so for SSIPs, which illustrates the dipolar alignment introduced by ion pairs in the solvent clusters. We now turn our attention to the implications of the structural properties of the ion pair clusters presented here for $NaI(H_2O)_n$ cluster photodissociation experiments.

4. Implications for $NaI(H_2O)_n$ photodissociation experiments

Our previous calculations of ion pair potentials of mean force and the resulting cluster ion pair equilibrium constants showed that the ion pairs are quite stable with respect to dissociation into free ions, even in very large clusters [53]. This can be attributed to the very slow convergence of cluster ion solvation energies to their bulk counterpart with increasing cluster size. Thus, separated cluster ions are thermodynamically very unlikely and ions rather tend to exist as CIP or SSIP, with the latter becoming thermodynamically predominant in the larger clusters (a feature which is nevertheless less pronounced at the low temperatures that experiments are likely to involve) [53]. Ab initio characterization of model cluster excited states suggested that $NaI(H_2O)_n$ cluster CIPs have optically accessible excited states akin to that of gas-phase NaI, hence making photodissociation experiments feasible, but that electronic transition oscillator strengths significantly decrease for model SSIPs, which become more likely with increasing cluster size [53]. As a result,

Table 4
Structural properties of SSIP $NaI(H_2O)_n$ clusters[a]

	$\langle R_{cm}\rangle$[b]	$\langle\Theta\rangle$[c]	$\langle I\rangle$[d]			$\langle\mu_T\rangle$[e]
n = 16 − OPLS						
	1.12 ± 0.38	77 ± 36	2390 ± 310	3530 ± 850	4190 ± 930	19.3 ± 2.8
n = 16 − OPCS						
	1.49 ± 0.56	77 ± 35	2560 ± 470	3930 ± 1110	4700 ± 1160	19.6 ± 3.4
n = 32 − OPLS						
Surface	1.37 ± 0.63	79 ± 35	7650 ± 720	10400 ± 1000	12100 ± 1250	23.4 ± 4.5
n = 32 − OPCS						
Interior	2.83 ± 0.48	94 ± 37	7760 ± 750	11100 ± 1320	13300 ± 1100	22.3 ± 4.1
Surface	1.80 ± 0.66	75 ± 32	7550 ± 690	10900 ± 1130	12800 ± 1310	20.4 ± 3.5

[a] The listed values are the average and the standard deviation of each structural property for ensembles of ≈5000 configurations generated at 300 K.
[b] Average distance (in Å) between the ion and the solvent cluster center of mass, as depicted in Fig. 8.
[c] Average angular position (in degrees) of the water molecules, as depicted in Fig. 8.
[d] Principal moments of inertia in amu Å^2.
[e] Total cluster dipole moment in D.

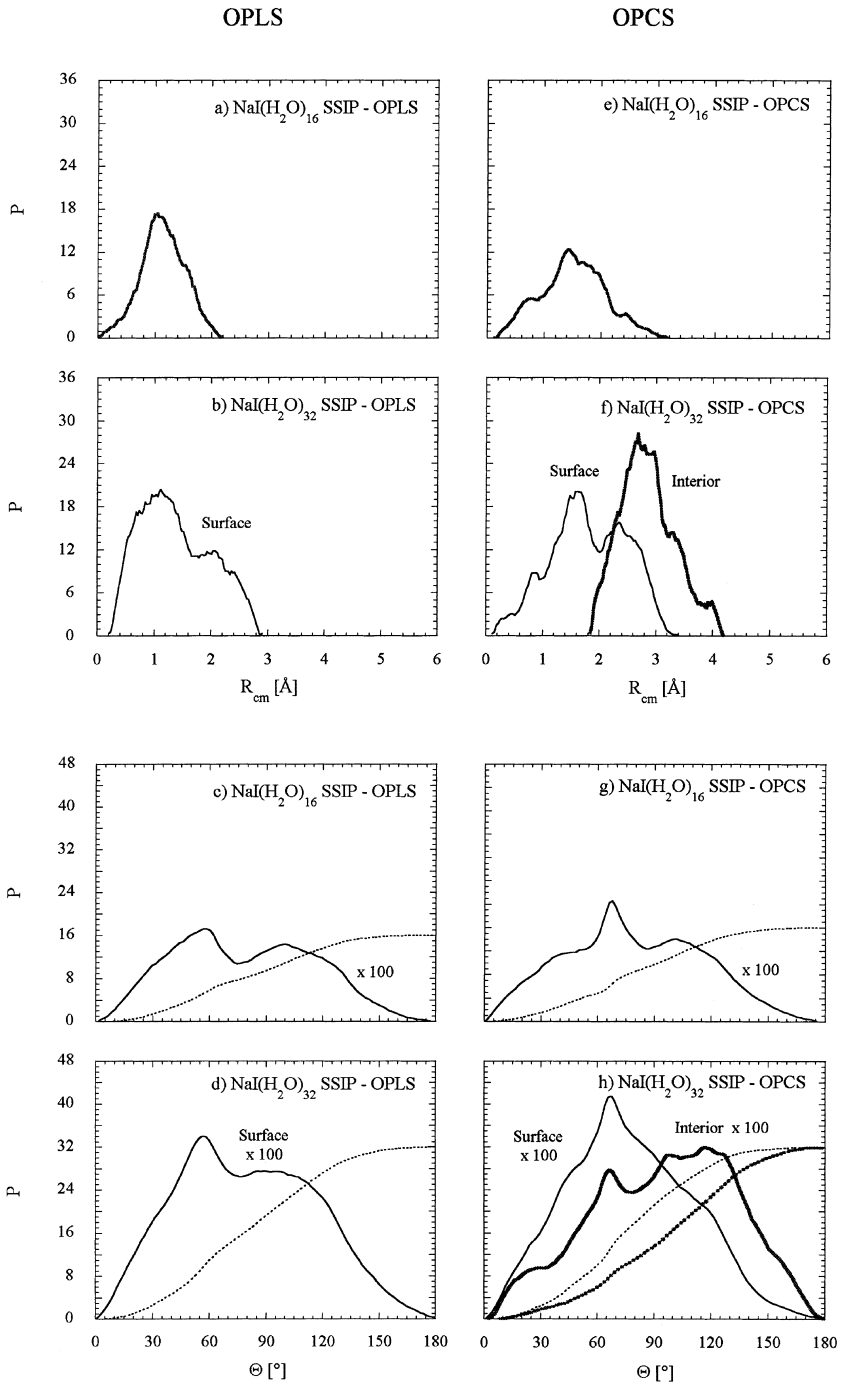

Fig. 12. $NaI(H_2O)_n$ SSIP cluster structural properties. Distributions of the R_{cm} and Θ coordinates of the water molecules for $n = 16$ and 32 with both OPLS and OPCS models. Also shown are the integral probabilities in dotted lines. The distributions are evaluated from ensembles containing ≈5000 configurations generated at 300 K.

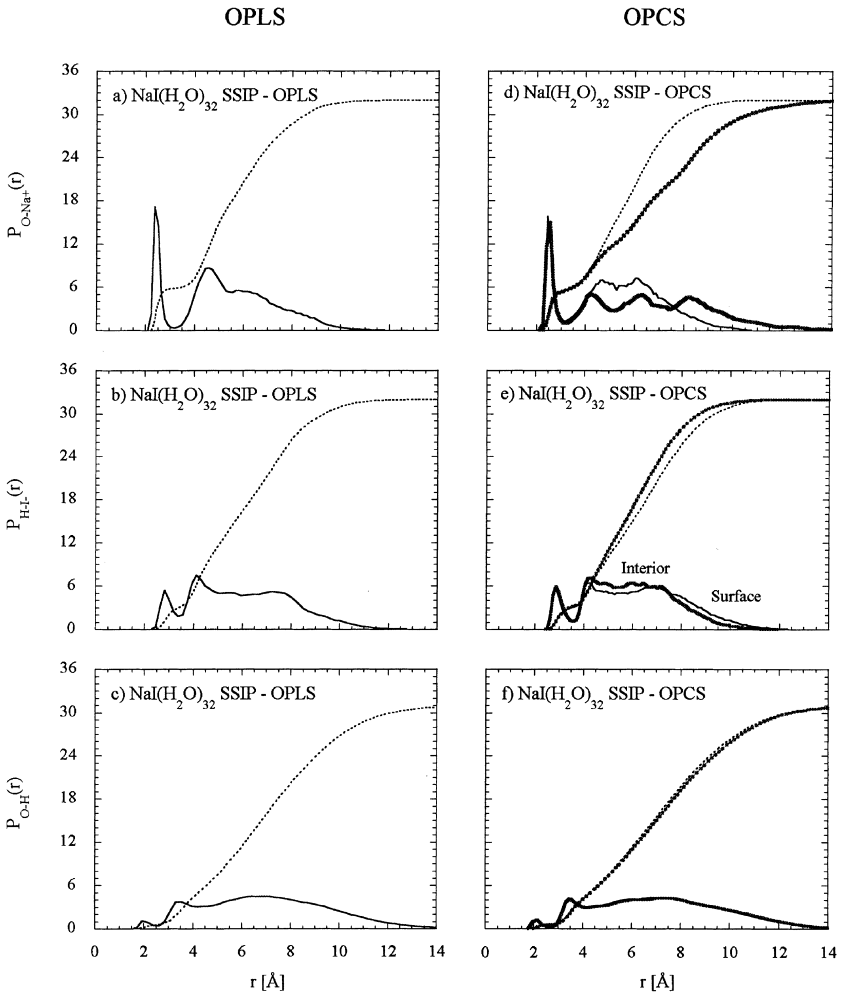

Fig. 13. $NaI(H_2O)_{32}$ SSIP cluster radial O–Na^+, H–I^- and O–H probability distributions with both OPLS and OPCS models. Also shown are the integral probabilities as dotted lines.

the larger (solvent-separated) cluster ion pairs may not be involved in cluster photodissociation reactions via a mechanism akin to gas-phase NaI photodissociation, in agreement with recent experimental findings. As a note of caution, we also add that large clusters may be difficult to generate in the experimental conditions [53]. [1]

The present results on the structural properties of the ion pair clusters may provide another possible explanation for the fact that large cluster products are not detected in photodissociation experiments. It is possible that the photoexcitation of the larger clusters proceeds via a different route than it does for the small clusters and isolated NaI. For example, as clusters grow, the net dipole moment of the whole water molecule network dramatically increases (and this feature is more pronounced for surface clusters), which is indicative of increasingly larger local alignment of solvent dipoles in the clusters. It is then conceivable that local water dipoles grow large enough to dipole bind an electron upon cluster photoexcitation, resulting in a charge-transfer-to solvent (CTTS) excited state with totally different dynamics from that of excited state NaI. Small clusters of iodide with water, acetone, or aceto-

nitrile, are known to possess such CTTS excited states [7–10].

Further, SSIPs exhibit a more pronounced surface-like character than do CIPs for large clusters, and the aforementioned CTTS mechanism that could shut down the perturbed isolated NaI photodissociation route becomes even more likely if water molecules arrange themselves around the iodide ion in a way to produce a large local solvent dipole as in $I^-(H_2O)_n$ surface clusters [7,8,60–64]. In that respect, SSIPs have much larger total solvent dipole moments than CIPs (as shown in Tables 3 and 4), and thus solvent arrangements with large local dipoles are even more likely for SSIPs. Along similar lines, SSIP structures resemble more those of $Na^+(H_2O)_n$ and $I^-(H_2O)_n$ clusters placed next to one another, as mentioned towards the end of Section 3.2, and the solvent structure being more akin to that of $I^-(H_2O)_n$ clusters around the iodide ion is more likely to dipole bind an electron upon photoexcitation. The CTTS mechanism may also be more likely for SSIPs than for CIPs, as the oscillator strength of the transition to an excited state akin to that of gas-phase NaI is much weaker for the former species [53].

Finally, we note that one of the major finding reported here, i.e. the surface structure of the small $NaI(H_2O)_n$ clusters, may imply for the NaI photodissociation pathway a slow convergence of the reaction dynamics of $NaI(H_2O)_n$ clusters with increasing cluster size [85]. As clusters grow, and water molecules more likely bond to each other rather than solvate the solute, the curve crossing dynamics characteristic of NaI photodissociation might not be so dramatically affected by the presence of more water molecules: the solvent mainly affects the curve crossing dynamics and the rate of non-adiabatic transitions by dynamically stabilizing the ion pair or the covalent NaI species, and the differential solvation energy between these states is rather insensitive to distant solvent molecules [44]. There is also less steric hindrance for the iodide/iodine to leave the cluster upon photoexcitation in surface structures (even though it is a heavy atom, compared to sodium or the water molecules), which is consistent with the experimental observation of large $Na^+(H_2O)_n$ cluster products.

5. Concluding remarks

We have investigated the structural properties of ion pair–water clusters that were predicted to be thermodynamically stable in previous work [53], by means of room-temperature Monte Carlo simulations with OPLS and OPCS model potentials. Considerable attention was also paid to the structure of the single ion-water clusters, which was revisited in a systematic fashion. Both $Na^+(H_2O)_n$ and $I^-(H_2O)_n$ clusters were shown to be non-spherically symmetric at room temperature. In agreement with earlier experimental [7,8] and theoretical [14,60–64] work, the $I^-(H_2O)_n$ clusters clearly exhibit surface structures, with the hydrophobic iodide ion sitting at the surface of a water molecule network. The $Na^+(H_2O)_n$ clusters on the other hand exhibit a solvation shell structure, with a first solvation shell of five to six water molecules. At low temperatures, the $Na^+(H_2O)_n$ clusters can possess spherically symmetric structures, such as cage-like structures reminiscent of a Buckyball or clathrates [23], but at room temperature, the sodium ion tends to be located towards the surface of the cluster: once the first solvation shell is complete, the solute–solvent interactions in the next solvation shell become weaker than the solvent–solvent interactions, and solvent molecules tend to accumulate on one side of the cluster instead of forming a spherical droplet. At large enough cluster sizes of course, entropy and long-range polarization effects may finally drive the ion towards the center of the cluster. A remarkable finding in this work is that room-temperature ion–water cluster structures are quite similar, whether one employs a non-polarizable potential derived for liquid simulations such as OPLS or a polarizable model geared towards the description of small clusters such as OPCS.

While both OPLS and OPCS predict quantitatively very different ion pair energetics and free energetics [53], they also predict rather similar structural properties for ion pairs in water clusters, even though some slight structural differences exist. Both the CIP and SSIP are found to have surface structures for the smaller clusters, while both interior and surface structures may exist at room temperature for cluster size of 32. Which one

of the interior or surface structures is the most thermodynamically likely for the larger $NaI(H_2O)_n$ clusters will be reported elsewhere [84], and both sets of cluster structures were presented separately in the present article. A striking feature of the ion pair cluster structural properties is that they are very much akin to those for individual ion–water clusters, especially for SSIPs, and we argue that some insight into the ion pair cluster structures can be gained from single ion–water cluster structures. In other words, most of the local solvent environment around the ions in $NaI(H_2O)_n$ CIP and SSIP clusters is quite similar to that in single ion–water $Na^+(H_2O)_n$ and $I^-(H_2O)_n$ clusters.

The solvent–solvent hydrogen bonding in ion-water and ion pair-water clusters was found to be rather small, and certainly smaller than in pure water clusters or in bulk water, due to the presence of solute species which strongly perturb the water molecule network. Along similar lines, the disorder introduced by the ions or ion pairs in the solvent network results in large values of the solvent cluster dipole moments. We suggest that both the extent of solvent–solvent hydrogen bonding and the magnitude of the solvent dipole moments could serve as a measure of the extent of the perturbation introduced by various solute species in solvent environments, and a detailed comparison of these quantities for solute-containing clusters and pure solvent clusters or even the liquid phase is left for future work [67].

Finally, the structures of the $NaI(H_2O)_n$ CIP and SSIP clusters have some implications for the cluster photodissociation dynamics. We showed earlier [53] that $NaI(H_2O)_n$ cluster CIPs are stable species with optically accessible excited states akin to that of gas-phase NaI, hence making photodissociation experiments feasible. The larger cluster ion pairs however, which are mainly SSIPs, may not be involved in cluster photodissociation reactions via a mechanism akin to gas-phase NaI photodissociation, as the oscillator strength of the electronic transition to the proper excited state is greatly reduced for SSIPs [53]. The structural properties of the ion pair clusters presented here may provide another possible explanation for the fact that large cluster products are not detected in photodissociation experiments (provided that parent clusters of large size can be generated under the experimental conditions [30]).[1] Photoexcitation of the larger clusters could proceed via a different route than it does for the small clusters and isolated NaI, possibly involving a CTTS excited state with totally different dynamics from that of excited state NaI, and akin to that of small clusters of iodide with water, acetone, or acetonitrile [7–10]. This idea is supported by the large solvent dipole moments obtained for $NaI(H_2O)_n$ clusters, a feature even more pronounced for surface clusters and SSIPs, which is indicative of increasingly larger alignment of solvent dipoles in the clusters. The dipoles resulting from this local alignment may then grow large enough to dipole-bind an electron upon cluster photoexcitation, initiating a CTTS mechanism that shuts down the perturbed NaI photodissociation pathway. Another implication of the structure of the small $NaI(H_2O)_n$ clusters, which are mainly surface structures, is that the photodissociation dynamics of $NaI(H_2O)_n$ may only converge slowly with increasing cluster size. As clusters grow and water molecules more likely bond to each other rather than solvate the solute, the curve crossing dynamics characteristic of NaI photodissociation pathway itself might not be so dramatically affected by the presence of more water molecules, resulting in a slow change of the $NaI(H_2O)_n$ cluster photodissociation dynamics with cluster size [85].

Acknowledgements

This research was supported in part by NSF grants CHE-9520619 and CHE-9981539 (B.M.L), NSF grant CHE-970049 (J.T.H), and by a grant from the Natural Sciences and Engineering Research Council (NSERC) of Canada (G.H.P).

References

[1] E.R. Bernstein (Ed.), Chemical Reactions in Clusters, Oxford University Press, New York, 1996.
[2] A.W. Castleman, K.H. Bowen, J. Phys. Chem. 100 (1996) 12911.
[3] P. Kebarle, Ann. Rev. Phys. Chem. 28 (1977) 445.
[4] A.W. Castleman, R.G. Keesee, Chem. Rev. 86 (1986) 589.
[5] J.V. Coe, Chem. Phys. Lett. 229 (1994) 161.

[6] J.V. Coe, J. Phys. Chem. A 101 (1997) 2055.
[7] D. Serxner, C.E.H. Dessent, M.A. Johnson, J. Chem. Phys. 105 (1996) 7231.
[8] P. Ayotte, C.G. Bailey, G.H. Weddle, M.A. Johnson, J. Phys. Chem. A 102 (1998) 3067.
[9] C.E.H. Dessent, C.G. Bailey, M.A. Johnson, J. Chem. Phys. 102 (1995) 6335.
[10] C.E.H. Dessent, C.G. Bailey, M.A. Johnson, J. Chem. Phys. 103 (1995) 2006.
[11] P. Perez, W.K. Lee, E.W. Prohofsky, J. Chem. Phys. 79 (1983) 388.
[12] G. Markovich, L. Perera, M.L. Berkowitz, O. Cheshnovsky, J. Chem. Phys. 105 (1996) 2675.
[13] T.N. Truong, E.V. Stefanovich, Chem. Phys. 218 (1997) 31.
[14] W.L. Jorgensen, D.L. Severance, J. Chem. Phys. 99 (1993) 4233.
[15] H. Kistenmacher, H. Popkie, E.J. Clementi, J. Chem. Phys. 61 (1974) 799.
[16] J.E. Combariza, N.R. Kestner, J. Jortner, Chem. Phys. Lett. 203 (1993) 423.
[17] J.E. Combariza, N.R. Kestner, J. Jortner, J. Chem. Phys. 100 (1994) 2851.
[18] D.S. Lu, S.J. Singer, J. Chem. Phys. 105 (1996) 3700.
[19] J.A. Draves, Z. Luthery-Schulten, W.-L. Liu, J.M. Lisy, J. Chem. Phys. 93 (1990) 4589.
[20] T.J. Selegue, N. Moe, J.A. Draves, J.M. Lisy, J. Chem. Phys. 96 (1992) 7268.
[21] O.C. Cabarcos, J.M. Lisy, Chem. Phys. Lett. 257 (1996) 265.
[22] C.J. Weinheimer, J.M. Lisy, J. Phys. Chem. 100 (1996) 15305.
[23] E.A. Steel, K.M. Merz, A. Selinger, A.W. Castleman, J. Phys. Chem. 99 (1995) 7829.
[24] H.D. Gai, L.X. Dang, G.K. Schenter, B.C. Garrett, J. Phys. Chem. 99 (1995) 13303.
[25] H.D. Gai, G.K. Schenter, L.X. Dang, B.C. Garrett, J. Chem. Phys. 105 (1996) 8835.
[26] S.H. Lee, J.C. Rasaiah, J. Phys. Chem. 100 (1996) 1420.
[27] D. Laria, R. Fernandez-Prini, Chem. Phys. Lett. 205 (1993) 260.
[28] D. Laria, R. Fernandez-Prini, J. Chem. Phys. 102 (1995) 7664.
[29] T. Asada, K. Nishimoto, Chem. Phys. Lett. 232 (1995) 518.
[30] I. Kusaka, Z.-G. Wang, J.H. Seinfeld, J. Chem. Phys. 108 (1998) 6829.
[31] B.J. Gertner, G.H. Peslherbe, J.T. Hynes, Isr. J. Chem. 40 (2000) 273.
[32] S.C. Tucker, D.G. Truhlar, J. Am. Chem. Soc. 112 (1990) 3347.
[33] B.J. Mason, The Physics of Clouds, second ed., Oxford University Press, London, 1971.
[34] H.R. Byers, Elements of Cloud Physics, University of Chicago Press, Chicago and London, 1965.
[35] N.H. Fletcher, The Physics of Rainclouds, University Press, Cambridge, 1962.
[36] P. Beichert, B.J. Finlayson-Pitts, J. Phys. Chem. 100 (1996) 15218.
[37] S. Langer, R.S. Pemberton, B.J. Finlayson-Pitts, J. Phys. Chem. A 101 (1997) 1277.
[38] D.O. DeHaan, B.J. Finlayson-Pitts, J. Phys. Chem. A 101 (1997) 9993.
[39] K.W. Oum, M.J. Lakin, D.O. DeHaan, T. Brauer, B.J. Finlayson-Pitts, Science 279 (1998) 74.
[40] C. George, J.L. Ponche, P. Mirabel, W. Behnke, V. Scheer, C. Zetzsch, J. Phys. Chem. 98 (1994) 8780.
[41] C. George, W. Behnke, V. Scheer, C. Zetzsch, L. Magi, J.L. Ponche, P. Mirabel, Geophys. Res. Lett. 22 (1995) 1505.
[42] F. Schweitzer, L. Magi, P. Mirabel, C. George, J. Phys. Chem. A 102 (1998) 593.
[43] G.H. Peslherbe, R. Bianco, J.T. Hynes, B.M. Ladanyi, J. Chem. Soc. Faraday Trans. 93 (1997) 977.
[44] G.H. Peslherbe, B.M. Ladanyi, J.T. Hynes, J. Phys. Chem. A 102 (1998) 4100.
[45] M.J. Rosker, T.S. Rose, A.H. Zewail, Chem. Phys. Lett. 146 (1988) 175.
[46] T.S. Rose, M.J. Rosker, A.H. Zewail, J. Chem. Phys. 88 (1988) 6672.
[47] T.S. Rose, M.J. Rosker, A.H. Zewail, J. Chem. Phys. 91 (1989) 7415.
[48] P. Cong, A. Mohktari, A.H. Zewail, Chem. Phys. Lett. 172 (1990) 109.
[49] A. Mohktari, P. Cong, J.L. Herek, A.H. Zewail, Nature 348 (1990) 225.
[50] P. Cong, G. Roberts, J.L. Herek, A. Mohktari, A.H. Zewail, J. Chem. Phys. 100 (1996) 7832.
[51] C. Jouvet, S. Martrenchard, D. Solgadi, C. Dedonder-Lardeux, M. Mons, G. Grégoire, I. Dimicoli, F. Piuzzi, J.P. Visticot, J.M. Mestdagh, P. Doliveira, P. Meynadier, M. Perdrix, J. Phys. Chem. 101 (1997) 2555.
[52] G. Grégoire, M. Mons, C. Dedonder-Lardeux, C. Jouvet, Eur. Phys. J. D 1 (1998) 5.
[53] G.H. Peslherbe, B.M. Ladanyi, J.T. Hynes, Free Energetics of Contact and Solvent-Separated NaI Ion Pairs in Water Clusters, J. Phys. Chem. A 104 (2000).
[54] J.L. Gao, J. Phys. Chem. 98 (1994) 6049.
[55] A.A. Chialvo, P.T. Cummings, J.M. Simonson, R.E. Mesmer, J. Mol. Liq. 73–4 (1997) 361.
[56] H. Piekarski, M. Tkaczyk, M. Bald, A. Szejgis, J. Mol. Liq. 73–4 (1997) 209.
[57] W.R. Fawcett, A.C. Tikanen, J. Mol. Liq. 73–4 (1997) 373.
[58] E. Guàrdia, R. Rey, J.A. Padró, Chem. Phys. 155 (1991) 187.
[59] L.X. Dang, J. Chem. Phys. 97 (1992) 1919.
[60] L. Perera, M.L. Berkowitz, J. Chem. Phys. 95 (1991) 1954.
[61] L. Perera, M.L. Berkowitz, J. Chem. Phys. 95 (1991) 4236.
[62] L. Perera, M.L. Berkowitz, J. Chem. Phys. 99 (1993) 4222.
[63] L.X. Dang, B.C. Garrett, J. Chem. Phys. 99 (1993) 2972.
[64] L.X. Dang, D.E. Smith, J. Chem. Phys. 99 (1993) 6950.
[65] W.L. Jorgensen, J. Chandrasekhar, J.D. Madura, R.W. Impey, M.L. Klein, J. Chem. Phys. 79 (1983) 926.
[66] L.X. Dang, T.-M. Chang, J. Chem. Phys. 106 (1997) 8149.

[67] D. Koch, G.H. Peslherbe, B.M. Ladanyi, J.T. Hynes, A Molecular Dynamics Study of Water Clusters and Liquid Water with a New Simple Polarizable Water Model, in preparation.
[68] M.P. Allen, D.J. Tildesley, Computer Simulation of Liquids, Oxford University Press, New York, 1989.
[69] J.H. Seinfeld, S.N. Pandis, Atmospheric Chemistry and Physics: From Air Pollution to Climate Change, Wiley, New York, 1998, pp. 569.
[70] J.K. Lee, J.A. Barker, F.F. Abraham, J. Chem. Phys. 58 (1973) 3166.
[71] H. Reiss, A. Tabazadeh, J. Talbot, J. Chem. Phys. 92 (1990) 1266.
[72] C.L. Weakliem, H. Reiss, J. Phys. Chem. 98 (1994) 6408.
[73] D.S. Lu, S.J. Singer, J. Chem. Phys. 103 (1995) 1913.
[74] R.L. Asher, D.A. Micha, P.J. Brucat, J. Chem. Phys. 96 (1992) 7683.
[75] J. Chandrasekhar, D.C. Spellmeyer, W.L. Jorgensen, J. Am. Chem. Soc. 106 (1984) 903.
[76] Y. Sakai, E. Miyoshi, T. Anno, Can. J. Chem. 70 (1992) 309.
[77] A.J. Hebert, F.J. Lovas, C.A. Melenders, C.D. Hollowell, T.L. Story, K. Street, J. Chem. Phys. 48 (1968) 2834.
[78] S.-S. Sung, P.C. Jordan, J. Chem. Phys. 85 (1986) 4045.
[79] S. Lin, P.C. Jordan, J. Chem. Phys. 89 (1988) 7492.
[80] G.H. Peslherbe, Semiempirical Molecular Dynamics Studies of Ion-Water Clusters: Free Energetics of Interior vs. Surface Solvation for $I^-(H_2O)_n$ Clusters, in preparation.
[81] A.A. Chialvo, P.T. Cummings, J. Chem. Phys. 105 (1996) 8274.
[82] L.S. Sremaniak, L. Perera, M.L. Berkowitz, Chem. Phys. Lett. 218 (1994) 377.
[83] M.J.S. Dewar, E.G. Zoebisch, E.F. Healy, J.J.P. Stewart, J. Am. Chem. Soc. 107 (1985) 3902.
[84] G.H. Peslherbe, B.M. Ladanyi, J.T. Hynes, Free Energetics of Interior vs. Surface Solvation for NaI Ion Pairs in Water Clusters, in preparation.
[85] G.H. Peslherbe, B.M. Ladanyi, J.T. Hynes, Nonadiabatic Trajectory Studies of the Photodissociation Dynamics of NaI in Small Water Clusters, in preparation.